Advanced Mechatronics Project Report

German University in Cairo
Mechatronics Engineering Department.

Amr Wael	Ahmed Hesham Khalaf	Eslam Moharam	Abdelrahman manea	Shehab elwakil
52-12977	*52-4429*	*52-5242*	*52-6907*	*52-11480*
T-28	*T-29*	*T-27*	*T-31*	*T-33*

***Abstract*—This project aims to design and implement a Twin Rotor Multi-Input Multi-Output (TR-MIMO) system, an essential benchmark for control system research. The TR-MIMO system presents multiple challenges due to its inherent coupling effect between the two rotors, making it a valuable platform for studying advanced control techniques, such as sliding-mode and predictive control. Our system is driven by Brushless DC Motors (BLDCs), controlled via Electronic Speed Controllers (ESCs), and powered by a Raspberry Pi 4. This proposal outlines the problem formulation, the mathematical modeling, and the required hardware components.**

***Index Terms*—Twin Rotor MIMO, Mechatronics, Coupled Systems, Control, Mathematical Modeling**

I. Literature Review

Because of nonlinear dynamics, significant cross-coupling effect, and underactuated nature, TRMS was built as a benchmark system where several different control strategies had been tried. Similar to a 2-DOF helicopter, this system can allow certain challenges in control precision between pitch and yaw dynamics and is therefore a very good platform to look into advanced control techniques.

Among the traditional control approaches, PID controllers have been widely used owing to their simplicity and large operating range [1]. However, PID controllers face some challenges related to nonlinear and coupled system tuning with very large overshoots and long settling times in most cases. On the other hand, MPC has been employed fairly effectively in constrained multivariable systems, though it is computationally hard for realtime applications [2],. Another modern approach is backstepping, which results in a systematic procedure for nonlinear control design but mainly depends on accurate system modeling and also involves intense computations.

SMC has been a robust alternative to deal with the challenges of TRMS. SMC is particularly useful if nonlinearities and external disturbances are considered since it constrains the system states to track a predefined sliding surface. One significant weakness with traditional SMC is something known as chattering-a high frequency in the control signal. Besides its effect on the control precision, chattering could further cause mechanical wear and potential damage in real time.

In this report, saturation functions will be applied to the sliding mode controller to avoid chattering. Using saturations in smoothing the switching action of the controller reduces oscillations without loss of robustness within the system. This will definitely ensure that the benefits accruable from SMC-including disturbance rejection and robust performance-are accrued while its main limitation is taken care of. The employment of the saturation function offers a pragmatic and effective approach to implementing SMC in the TRMS and thus is a promising solution toward the intrinsic control challenges in this system.

This paper is on the realization of Sliding Mode Control together with a saturation technique for chattering elimination and further performance enhancement of the TRMS controller. Other techniques such as PID, MPC, and backstepping are used for insight and comparison; all these techniques are subsidiary in SMC due to its robustness and adaptability for nonlinear coupled dynamics.

II. Introduction

The Twin Rotor Multi-Input Multi-Output (TR-MIMO) system is a complex, nonlinear system that closely resembles the dynamics of a helicopter. It consists of two rotors: one for pitch control (vertical motion) and one for yaw control (horizontal motion). However, unlike simpler systems, the motion of one rotor affects the other, introducing a coupling effect between the two axes.[2]

Fig. 1. Twin-Rotor-MIMO-System

III. Problem Formulation

The objective of the TR-MIMO system is to control both the yaw and pitch angles using two BLDC motors. Each rotor's motion is governed by its own dynamics, but they are coupled due to gyroscopic motion.[3]

We define the following variables:

- ψ: Pitch angle
- ϕ: Yaw angle
- τ_1: Torque generated by the pitch motor
- τ_2: Torque generated by the yaw motor

The goal is to develop a control strategy that regulates θ_y and θ_p, while compensating for the interaction between the two motions.

IV. Mathematical Modeling

The mathematical model of the Twin Rotor Multi-Input Multi-Output (TR-MIMO) system accounts for the dynamic interactions between the pitch and yaw axes. The following equations describe the system's dynamics, including coupling effects.

A. Vertical Plane Motion

The motion in the vertical plane (pitch axis) is governed by the equation: [1]

$$I_1\ddot{\psi} = M_1 - M_{FG} - M_{BV} - M_G \tag{1}$$

where:

$$M_1 = a_1 \cdot \tau_1^2 + b_1 \cdot \tau_1, \quad \text{(nonlinear static characteristic)} \tag{2}$$

$$M_{FG} = M_s \cdot \sin\psi, \quad \text{(gravity momentum)} \tag{3}$$

$$M_{BV} = B_{1\psi} \cdot \dot{\psi} + B_{2\psi} \cdot \sin(\dot{\psi}), \quad \text{(friction forces momentum)} \tag{4}$$

$$M_G = K_g \cdot M_1 \cdot \dot{\phi} \cdot \cos\psi, \quad \text{(gyroscopic momentum)} \tag{5}$$

1) Motor Dynamics in the Vertical Plane: The motor momentum in the vertical plane is described by an approximated first-order transfer function in the Laplace domain:

$$\tau_1 = \frac{k_1}{T_{11}s + T_{10}} \cdot u_1 \tag{6}$$

B. Horizontal Plane Motion

The motion in the horizontal plane (yaw axis) is governed by the equation:

$$I_2\ddot{\phi} = M_2 - M_{B\phi} - M_R \tag{7}$$

where:

$$M_2 = a_2 \cdot \tau_2^2 + b_2 \cdot \tau_2, \quad \text{(nonlinear static characteristic)} \tag{8}$$

$$M_{B\phi} = B_{1\phi} \cdot \dot{\phi} + B_{2\phi} \cdot \sin(\dot{\phi}), \quad \text{(friction forces momentum)} \tag{9}$$

1) Cross Reaction Momentum: The cross-reaction momentum, which describes the coupling between the vertical and horizontal planes, is approximated by:

$$M_R = \frac{k_r(T_s s + 1)}{(T_s s + 1)} \cdot \tau_1 \tag{10}$$

2) Motor Dynamics in the Horizontal Plane: Similarly, the motor momentum in the horizontal plane is given by: [4]

$$\tau_2 = \frac{k_2}{T_{21}s + T_{20}} \cdot u_2 \tag{11}$$

V. Sliding Mode Control (SMC)

In contrast to alternative nonlinear control approaches, Sliding Mode Control (SMC) exhibits greater resilience to internal parameter fluctuations and external disturbances once the system trajectory stabilizes on the sliding surface. Nevertheless, the pivotal challenge lies in crafting an SMC controller that minimizes chattering, prompting our pursuit of a novel reaching law discussed in the subsequent section. For a comprehensive exploration of SMRL theory, refer to [**?**]. This section offers a concise introduction to the fundamental SMC design methodology.

Typically, SMC design entails two primary steps: first, selecting the sliding-mode surface, followed by devising the control input to steer the system trajectory towards this surface. This strategy guarantees the system's adherence to the sliding-mode reaching condition, articulated as follows:[3]

$$s \cdot \dot{s} < 0 \tag{12}$$

where s is the sliding-mode surface.

The following second-order nonlinear model is generally used to describe the SMC system adopting one reaching law method:

$$\dot{x}_1 = x_2 \tag{13}$$

$$\dot{x}_2 = f(x) + g(x) + b(x)u \tag{14}$$

where $x = [x_1, x_2]^T$ is the system state, $g(x)$ represents the system disturbances, and $b(x) \neq 0$.

The concrete steps include the following. First, the typical sliding-mode surface is chosen as follows:

$$s_1 = cx_1 + x_2 \tag{15}$$

Such a sliding-mode surface can guarantee the asymptotic stability of the sliding mode, and the asymptotic rate of convergence is in direct relation with the value of c. Next, the control input u should be designed in such a way as to ensure that the sliding-mode reaching condition outlined in inequality (2.1) is satisfied. Therefore, the equal reaching law is commonly selected in the following manner:

$$\dot{s}_1 = -k_1 \cdot \text{sgn}(s_1) \tag{16}$$

Substituting (2.3) into (2.4) yields

$$c\dot{x}_1 + \dot{x}_2 = -k_1 \cdot \text{sgn}(s_1) \tag{17}$$

Next, substituting (2.2) into (2.5) yields

$$cx_2 + f(x) + g(x) + b(x)u = -k_1 \cdot \text{sgn}(s_1) \tag{18}$$

Then, according to (2.6), the control input u can be easily expressed as

$$u = -b^{-1}(x)\big[cx_2 + f(x) + g(x) + k_1 \cdot \text{sgn}(s_1)\big] \tag{19}$$

In this context, the presence of the discontinuous term $-b^{-1}(x)k_1 \cdot \text{sgn}(s_1)$ in the control input results in chattering. The intensity of chattering is directly linked to the value of k_1.

The duration needed to reach the sliding-mode surface can be calculated by integrating equation (2.4) over time in the following manner:

$$t_1 = \frac{|s(0)|}{k_1} \tag{20}$$

The reaching time can be adjusted directly by the value of k_1. Increasing the value of k_1 results in a quicker reaching time and enhanced robustness. However, this also leads to a higher level of chattering in the control input. For our multi input multi output system we will introduce two sliding surfaces.

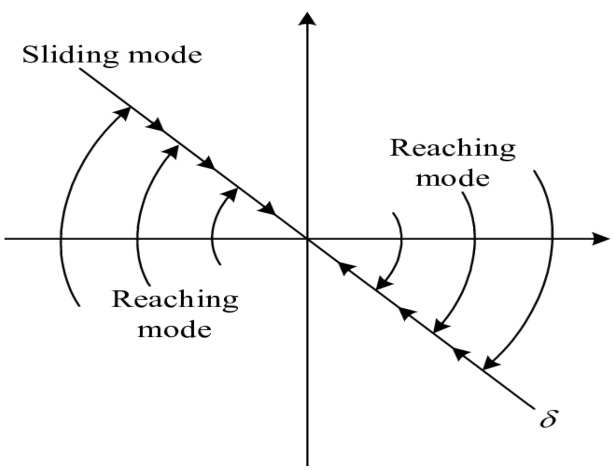

Fig. 2. Sliding-mode mechanism in phase plane.

VI. Simulations and Results

A. Open Loop

As illustrated in Fig. 3, the twin-rotor system consists of two open-loop input signals controlling the pitch and yaw movements of the rotor blades independently. As shown in Fig. 4, the open-loop response demonstrates the behavior when an input voltage is applied to both the main rotor and the tail rotor. It can be observed that the tail rotor exhibits instability during the response.

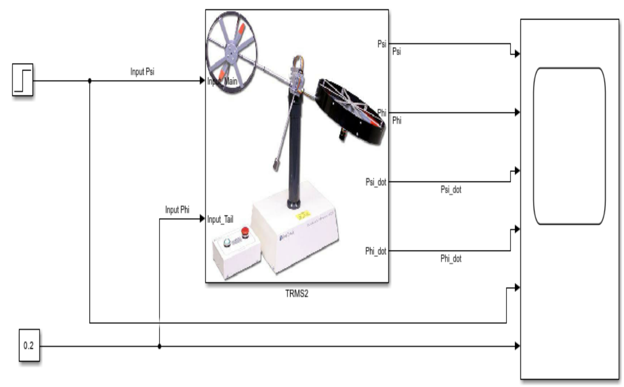

Fig. 3. SIMULINK model for twin rotor system.

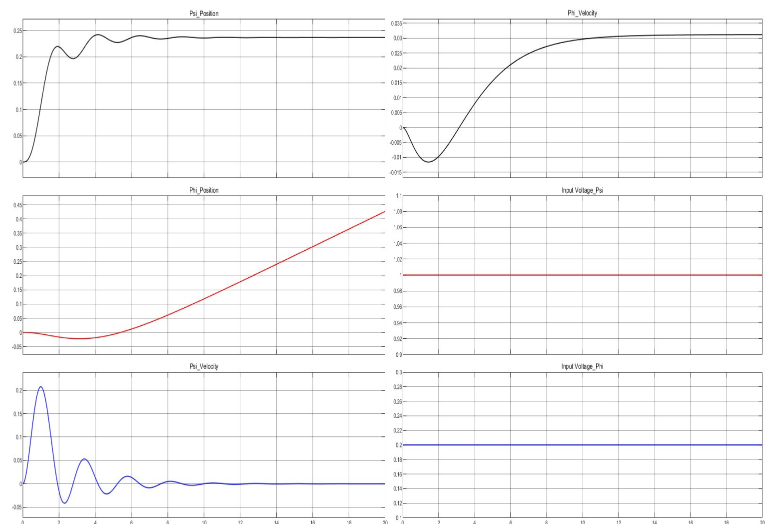

Fig. 4. Response of open loop system when 2 inputs applied to main and tail rotors.

As shown in Fig. 14, the output response of the system is presented when a step input is applied solely to the main rotor. It can be observed that the coupling effect between the main rotor and the tail rotor leads to noticeable interactions in the tail rotor's behavior.

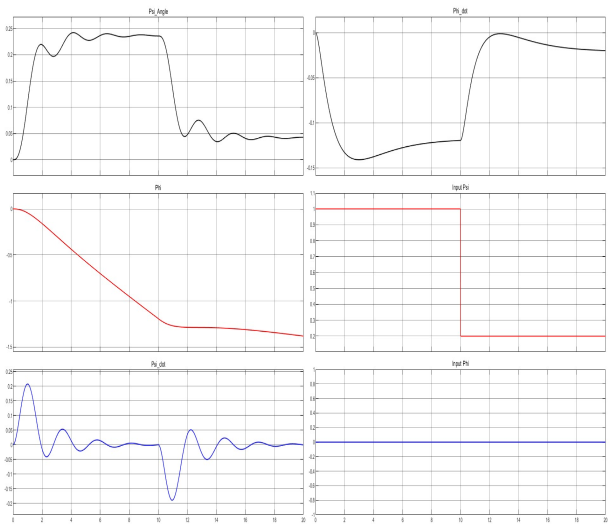

Fig. 5. Response of open loop system when only main input is applied.

B. Closed Loop

Figure 6 illustrates the closed-loop system with sliding mode control applied to both the pitch and yaw angles, using the inputs to the main and tail rotors of the system.

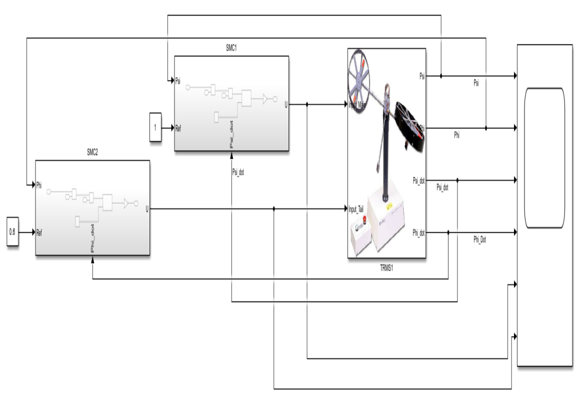

Fig. 6. Closed Loop system with sliding mode control.

Figure 8 illustrates the response of the twin rotor system after applying a step input in the presence of sliding mode control. It demonstrates how the sliding mode effectively mitigates the disturbance effect of the main rotor on the tail rotor. Additionally, with the inclusion of the saturation function, a significant reduction in chattering can be observed.

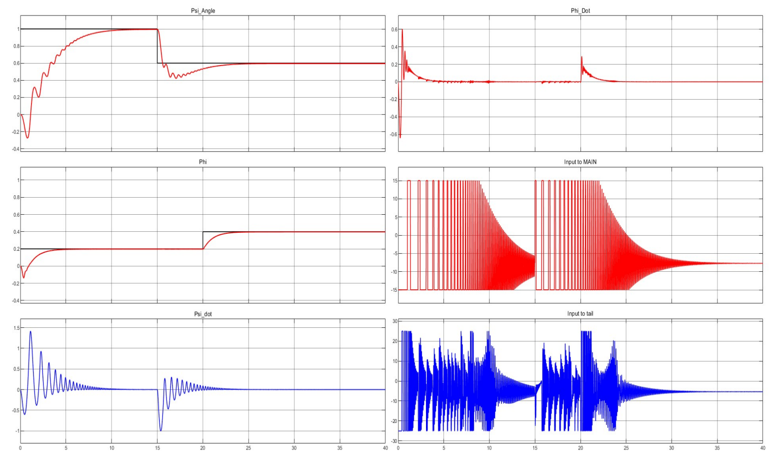

Fig. 7. Response of the closed-loop system when two step inputs are applied to the main and tail rotors.

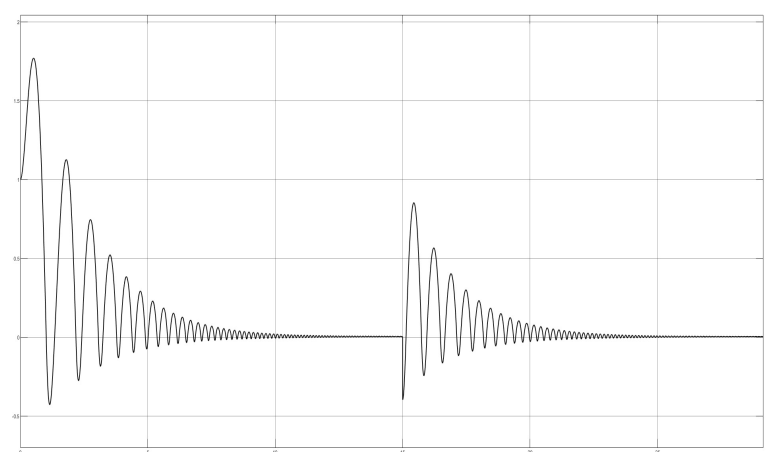

Fig. 8. Sliding surface of the main trajectory.

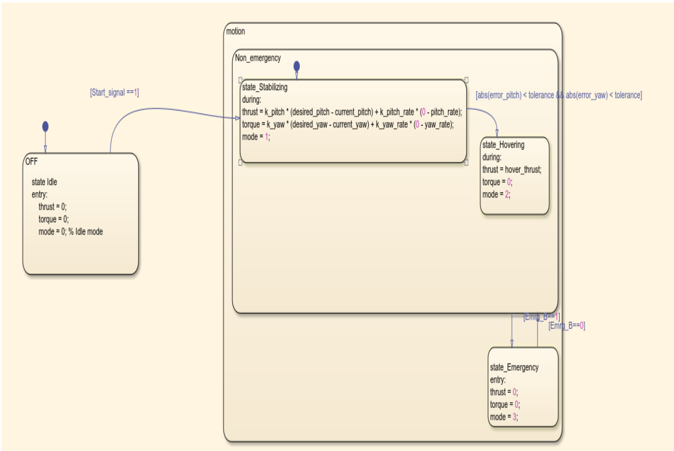

Fig. 9. State flow diagram of our System.

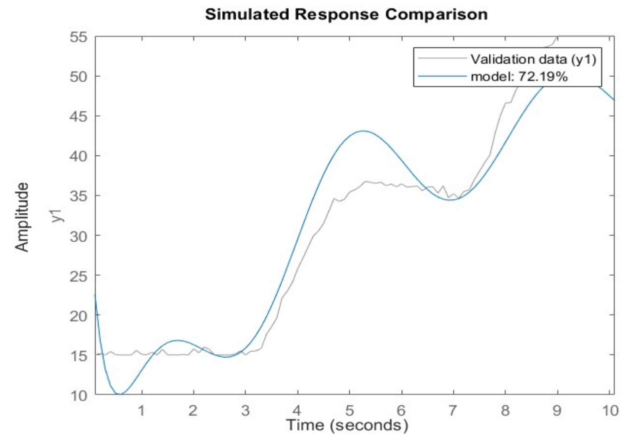

Fig. 11. Validation Output of the input to the main to the pitch angle

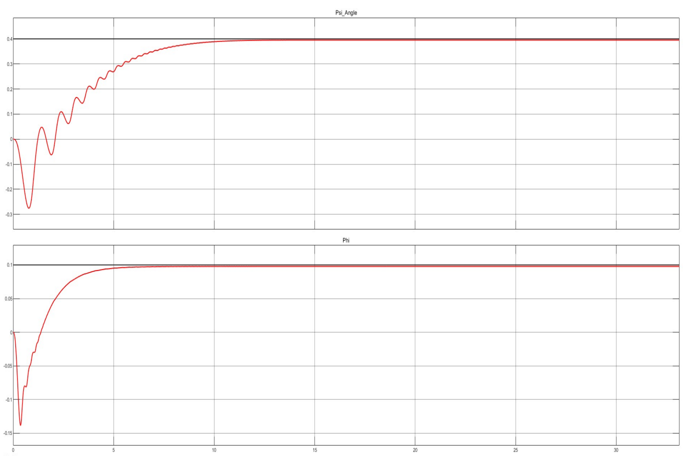

Fig. 10. Output of the system using the state flow discrete system.

In **Fig.13**, we present the discrete model of our system designed for stabilization. The model incorporates three key states: *stabilization*, *hovering*, and *emergency*. The stabilization state ensures that the desired angle is maintained. If the desired angle is not achieved, the stabilization mechanism generates a sliding mode control (SMC) input, which is transmitted to the motors through the hovering state. The hovering state manages the system's steady position while serving as a relay. The emergency state is included to ensure the safety of the system in case of critical situations.

VII. System Identification of the Twin Rotor MIMO System

In the analysis of the Twin Rotor MIMO System, the following transfer functions (TFs) were identified for various conditions when a voltage was applied to the main and tail rotors:

Pitch Angle Response (Main Rotor Input)

The transfer function for the pitch angle response when a voltage is applied to the main rotor is given by:

$$\mathrm{TF}_{\text{pitch}}(s) = \frac{0.0045}{s^4 + 3.1372s^3 + 4.3341s^2 + 7.5601s + 3.4150 \times 10^{-10}}$$

This transfer function models the dynamic behavior of the system in response to the main rotor input for pitch angle.

Yaw Angle Response (Main Rotor Input)

When the voltage is applied to the main rotor, the transfer function for the yaw angle response is:

$$\mathrm{TF}_{\text{yaw, main}}(s) = \frac{0.0054s + 8.1011 \times 10^{-4}}{s^2 + 0.1945s + 0.0082}$$

This TF represents the yaw angle behavior influenced by the main rotor input.

Yaw Angle Response (Tail Rotor Input)

When the voltage is applied to the tail rotor, the transfer function for the yaw angle response is:

$$\mathrm{TF}_{\text{yaw, tail}}(s) = \frac{0.0054s + 0.0020}{s^2 + 0.5192s + 2.4877 \times 10^{-8}}$$

This transfer function represents the yaw angle response when the tail rotor is the input.

These transfer functions provide valuable insight into the system dynamics and are essential for further control design and system analysis.

VIII. Hardware

A. Components

The system uses the following hardware components:

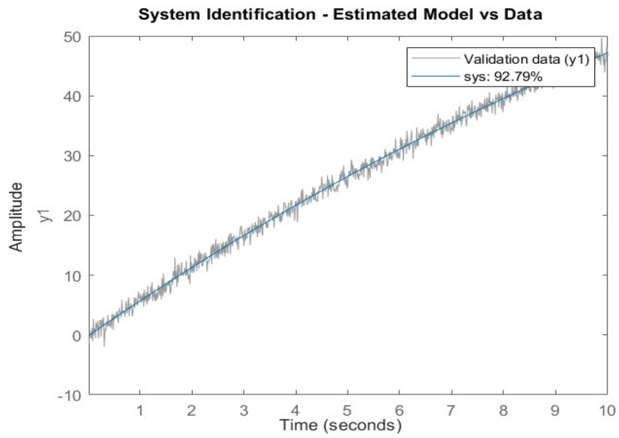

Fig. 12. Validation Output of the input to the main to the yaw angle

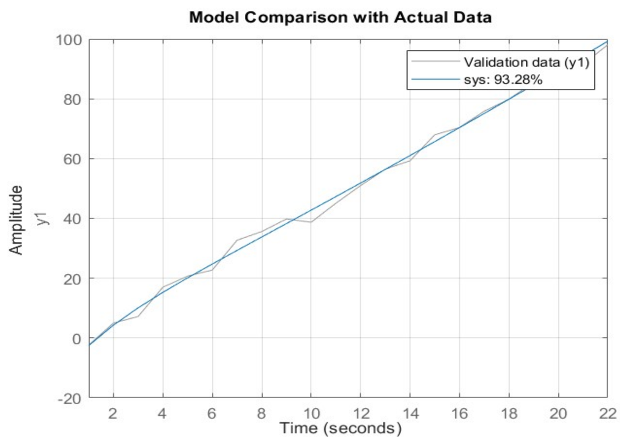

Fig. 13. Validation Output of the input to the tail rotor to the yaw angle.

B. Component Functionality

- **Raspberry Pi 4**: Acts as the main processing unit, handling sensor input and motor control algorithms.
- **BLDC Motors**: Control the yaw and pitch motion of the rotors.
- **ESCs**: Interface between the Raspberry Pi and the BLDC motors, controlling motor speed based on PWM signals.
- **IMU Sensors**: Measure angular velocities and accelerations, providing feedback for real-time control.
- **Breadboard**: Used to connect sensors, ESCs, and other components to the Raspberry Pi.
- **12V Li-ion Battery**: Provides the necessary power for the system, including motors and electronics.

TABLE I
LIST OF HARDWARE COMPONENTS

Component	Quantity
Raspberry Pi 4	1
BLDC Motor	2
Electronic Speed Controller (ESC)	2
IMU Sensor	2
Breadboard	1
12V Li-ion Battery	1

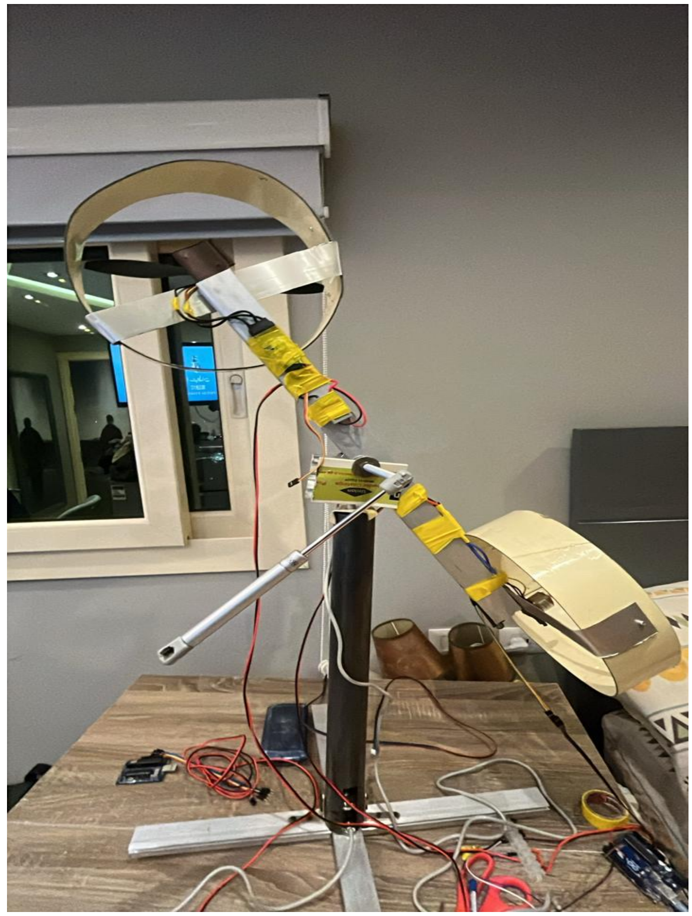

Fig. 14. Our Hardware Model.

IX. REFERENCES

[1] D. M. Ezekiel, R. Samikannu, and M. Oduetse, "Modelling of the Twin Rotor MIMO System (TRMS) Using the First Principles Approach," in *2020 International Conference on Computer Communication and Informatics (ICCCI) [2] [Lidia Belmonte Rafael Morales]. [20 Oct 2024]. Robust Decentralized Nonlinear Control for a Twin Rotor MIMO System. Scientific Figure on ResearchGate. [3] Ranjan, K. V., Laxmi, V. (2022). Design of an optimal controller for a Twin Rotor MIMO System (TRMS). In 2022 International Conference on Sustainable Computing and Data Communication Systems (ICSCDS) (pp. 950-959). Erode, India. [4] Huong*, Nguyen T. M. "Model Predictive Control for Twin Rotor Mimo System (Trms)." The University of Danang- Journal of Science and Technology, no. 1, 2014, pp. 39-42